Object crowding in age-related macular degeneration

Julian M. Wallace
Department of Psychology, University of Southern California, Los Angeles, CA, USA

Susana T. L. Chung
School of Optometry, University of California, Berkeley, Berkeley, CA, USA

Bosco S. Tjan
Department of Psychology, University of Southern California, Los Angeles, CA, USA
Neuroscience Graduate Program, University of Southern California, Los Angeles, CA, USA

Crowding, the phenomenon of impeded object identification due to clutter, is believed to be a key limiting factor of form vision in the peripheral visual field. The present study provides a characterization of object crowding in age-related macular degeneration (AMD) measured at the participants' respective preferred retinal loci with binocular viewing. Crowding was also measured in young and age-matched controls at the same retinal locations, using a fixation-contingent display paradigm to allow unlimited stimulus duration. With objects, the critical spacing of crowding for AMD participants was not substantially different from controls. However, baseline contrast energy thresholds in the noncrowded condition were four times that of the controls. Crowding further exacerbated deficits in contrast sensitivity to three times the normal crowding-induced contrast energy threshold elevation. These findings indicate that contrast-sensitivity deficit is a major limiting factor of object recognition for individuals with AMD, in addition to crowding. Focusing on this more tractable deficit of AMD may lead to more effective remediation and technological assistance.

Introduction

People with age-related macular degeneration (AMD) lose their central visual field and must rely on peripheral vision for their daily activities, which is often difficult. One reason for this difficulty may be due to crowding, which impairs object recognition in a cluttered environment and is prominent in normal peripheral vision. To date, most published reports on crowding in AMD participants were obtained using tasks of letter recognition or reading (Chung, Jarvis, Woo, Hanson, & Jose, 2008; Chung, 2013, 2014; Calabrèse et al., 2010). The present study extends the work of Wallace and Tjan (2011) on object crowding to participants with AMD. We specifically tested AMD participants who have adopted a stable preferred retinal locus (PRL) for fixation.

Crowding refers to the phenomenon with which stimuli become harder to identify when flanked by other objects (Bouma, 1970; Andriessen & Bouma, 1976; Levi, 2008; Pelli & Tillman, 2008; Whitney & Levi, 2011). In normally sighted individuals, this effect is more prominent in the peripheral field, over and above any other detrimental effect peripheral vision has on simple detection of targets. A hallmark of crowding is its dependence on eccentricity—the minimum distance between target and flanker stimuli that causes impaired identification depends upon the eccentricity in the visual field. This critical spacing is approximately a constant fraction of the eccentricity of the peripheral target (Bouma, 1970, 1973). A scaling factor of half the eccentricity is commonly referred to as Bouma's law although others find lower scaling values (e.g., Strasburger, Harvey, & Rentschler, 1991; Chung, Levi, & Legge, 2001). Crowding and its spatial extent (or crowding zone), defined by the critical spacing, have been studied extensively with simple visual stimuli, such as Gabors and letters (Andriessen & Bouma, 1976; Toet & Levi, 1992; He, Cavanagh, & Intriligator, 1996). The same effect also holds when viewing natural stimuli of the kind we encounter when carrying out our daily life, such as objects (Pelli & Tillman, 2008; Wallace & Tjan, 2011), faces (Martelli, Majaj, & Pelli, 2005; Louie, Bressler, & Whitney, 2007; Farzin, Rivera, & Whitney, 2009), and biological motion (Ikeda, Watanabe, & Cavanagh, 2013). Crowding is known to occur

Citation: Wallace, J. M., Chung, S. T. L., & Tjan, B. S. (2017). Object crowding in age-related macular degeneration. *Journal of Vision*, *17*(1):33, 1–12, doi:10.1167/17.1.33.

doi: 10.1167/17.1.33 Received August 4, 2015; published January 27, 2017 ISSN 1534-7362

beyond retinal processing (Flom, Heath, & Takahashi, 1963), and the effect is generally attributed to anomalous integration of features (Levi, Hariharan, & Klein, 2002; Pelli et al., 2004; Nandy & Tjan, 2007) although the precise mechanism remains elusive. Crowding can be thought of as an information-processing bottleneck, and on a fundamental level, it has the potential to provide insight into general mechanisms of form processing and object recognition (Levi, 2008; Pelli & Tillman, 2008; Nandy & Tjan, 2012).

Without a functioning fovea, patients with AMD often adopt a peripheral retinal location, the PRL, for fixation (Cummings, Whittaker, Watson, & Budd, 1985; Schuchard & Fletcher, 1994). The extensive use of the peripheral PRL may lead to a substantial reduction of crowding at the PRL. Whether or not there is a substantial reduction in crowding at the PRL has important implications for clinical practice as well as our understanding of peripheral form vision. If crowding remains a dominant limiting factor at the PRL, it would be important to consider various methods for reducing visual crowding as aids to AMD patients. Alternatively, investing in treatments that improve other aspects of peripheral vision, such as fixation stability or treating the pathologies in the periphery that may improve contrast sensitivity or acuity, may be more effective. Furthermore, if crowding remains prominent at the PRL despite extensive use of the peripheral location for form vision, it would also imply that the underlying mechanism of crowding is related to a hardwired aspect of the peripheral visual system that cannot be easily modified.

A recent study has provided some intriguing results. Chung (2013) measured the crowding zone using a standard letter recognition task for adult participants with macular disease and stable PRL and compared these with age-matched control participants with normal vision. Eight of her 11 participants had AMD. The shape of the peripheral crowding zones for the normal control participants exhibited the typical radial–tangential anisotropy elongated along the radial direction. Surprisingly, although the participants with macular disease had a similar size of crowding zone in the tangential direction at the PRL, the extent of the zone was reduced in the radial direction. In other words, Chung (2013) found that the crowding zone at the PRL of individuals with macular disease was less elongated, resembling the roundish shape of the crowding zone associated with foveal crowding in normally sighted individuals.

With a smaller (less elongated) crowding zone at the PRL, do patients with macular disease have better form vision at the PRL? The present study provides a characterization of object crowding with binocular viewing at the PRL of three AMD participants with varying degrees of visual deficits and compares their performance to that of both age-matched and young controls. This extends the work of Wallace and Tjan (2011), who measured critical spacing for objects (photographs of real-world objects) and compared it to that for standard letter crowding. Wallace and Tjan found that although critical spacing was similar for both stimulus types, the strength of crowding, measured in terms of contrast elevation, was much less for objects. By characterizing crowding in terms of critical spacing and contrast threshold elevation, we obtained a more comprehensive assessment of form vision in clutter. The present study provides the first such characterization of object crowding at the PRL of AMD participants. To anticipate the results, we found that critical spacing for object recognition in AMD participants was not substantially different from that of aged-matched and young controls when tested at the same location corresponding to the PRL of an AMD participant by way of a gaze-dependent stimulus presentation method. However, we also found that the contrast sensitivity for identifying isolated objects was far worse in AMD participants compared to controls. Additionally, threshold elevation due to crowding was worse for the AMD participants as compared to controls.

Methods

Participants

Three participants with long-standing AMD participated in this study. Table 1 lists the characteristics of these three participants. All had a well-developed PRL for fixation as assessed using a Rodenstock 101 scanning laser ophthalmoscope (SLO). Figure 1 shows, for each AMD participant, the PRL location and the approximate coverage of the central absolute scotoma of the preferred eye most likely used to view the stimuli in our binocular testing as well as those from the nonpreferred eye. AMD is a bilateral disease but typically with one eye demonstrating a more advanced form. In this study, we defined the preferred eye based upon participants' report, which corresponded to the eye with better acuity for two of the three AMD participants (Table 1). We relied on self-report because test–retest reliability of acuity measurement in patients with central vision loss is about two 2 lines (0.2 logMAR; Patel, Chen, Rubin, & Tufail, 2008), close to the acuity difference in some of our participants. (Note that S2 chose what seemed to be her worse eye as her preferred eye. One possibility is that it had been S2's preferred eye since the onset of AMD, and given that

	Acuity (logMAR)			Fixation stability	
Observer	OS	OD	Years since onset	Horizontal *SD* (°)	Vertical *SD* (°)
S1	0.48*	0.66	7	0.95	0.20
S2	0.52	0.50*	9	0.32	0.33
S3	0.74*	0.70	11	0.72	0.50

Table 1. Visual characteristics of the three participants with AMD. *Notes*: *Preferred eye of each participant based on self-reports. Fixation stability refers to the eye positions measured monocularly with the preferred eye using the SLO during trials of 30 s of fixation.

acuity only differed by one letter between the two eyes, S2 still preferred to use that eye over the other eye.)

Testing of the AMD participants was conducted at the University of California, Berkeley. The three participants all had substantial experience with psychophysics experiments and gave oral and written consent before the commencement of data collection. Procedures for testing these patients were approved by the Institutional Review Board at the University of California, Berkeley.

Six (three young and three elderly) control participants were tested at a retinal location equivalent to the PRL of the AMD participants to whom they were matched (see Table 2). Testing of the normal control participants was performed at the University of Southern California (USC), and the protocol was approved by the Institutional Review Board of USC.

Stimuli

We used 20 target objects and 20 different flanker objects. All objects were grayscale photographs of objects and were a subset of those used in Wallace and Tjan (2011); details of the initial stimulus selection process can be found in that paper. All objects were matched in height but variable in width. Objects were equalized for root-mean-square (RMS) contrast (0.21 for all objects). Contrast equalization did not change the mean luminance of an object. We manipulated the contrast of these contrast-equalized objects in the experiments, and the "nominal" contrast was defined as 100% when their RMS contrast was 0.21 (the maximum contrast level without luminance clipping). The average complexity (ratio of squared perimeter to area) of both targets and flankers was almost identical (target mean complexity = 25.45; flanker mean complexity = 26.33) with a range from 15.39 to 44.67.

The flankers were always presented at 50% nominal contrast and arranged horizontally on the screen relative to the target object for both AMD and control participants at all tested eccentricities. The stimulus size was determined by estimating the acuity object size required for recognition of isolated targets by the AMD participants at an accuracy of 50% after correction for guessing (5%); a size twice that of the acuity object size was then used for testing the AMD participant and for the controls matched to that AMD participant. This object size was held constant throughout the experiment. The object sizes (in term of object height) used for the AMD participants and corresponding control participants were 1.47° (S1), 1.32° (S2), and 2.36° (S3). At these object sizes, the AMD and control participants could perfectly identify the target objects when presented alone at 100% nominal contrast.

Procedures

Following Wallace and Tjan (2011), we used QUEST (Watson & Pelli, 1983) to measure contrast thresholds for 75% target identification accuracy over a range of target–flanker spacing. The method allows us to estimate two key parameters: the critical spacing, the distance at which flankers begin to have a deleterious effect on threshold performance, and threshold elevation, the extra amount of target contrast that is required above baseline level to attain the same recognition performance when the flankers are close to the target (see Analysis section for further explanation). At small target–flanker spacing, objects could overlap with one another. When that happened, the target was always presented in front of the flankers, occluding the flankers (Figure 7). The target was never occluded.

Targets were randomly chosen from the set of 20 objects (grayscale photographs), and flankers were randomly chosen from a different set of 20 objects. Participants viewed the stimulus with unlimited viewing time. The target (center object) was positioned at the center of the display, indicated by markers placed above and below it. Control participants were tested with a similar procedure at an eccentric retinal location matching the PRL of one of the three AMD participants. To allow for unlimited viewing time for control participants, an eye tracker was used to monitor fixation, and the stimulus was turned off whenever fixation strayed from the fixation mark by more than 1.5°.

AMD and control participants viewed the stimulus binocularly with appropriate corrections for the viewing distance. Binocular viewing is the natural mode of seeing for AMD participants. Assessment of functional vision in AMD is thus best done with binocular viewing. In AMD, binocular viewing also results in better gaze control (Tarita-Nistor, Brent, Steinbach, & González, 2012) and thus better fixation stability. For the AMD participants at Berkeley, the PRL was assumed to be the one from their preferred eye based

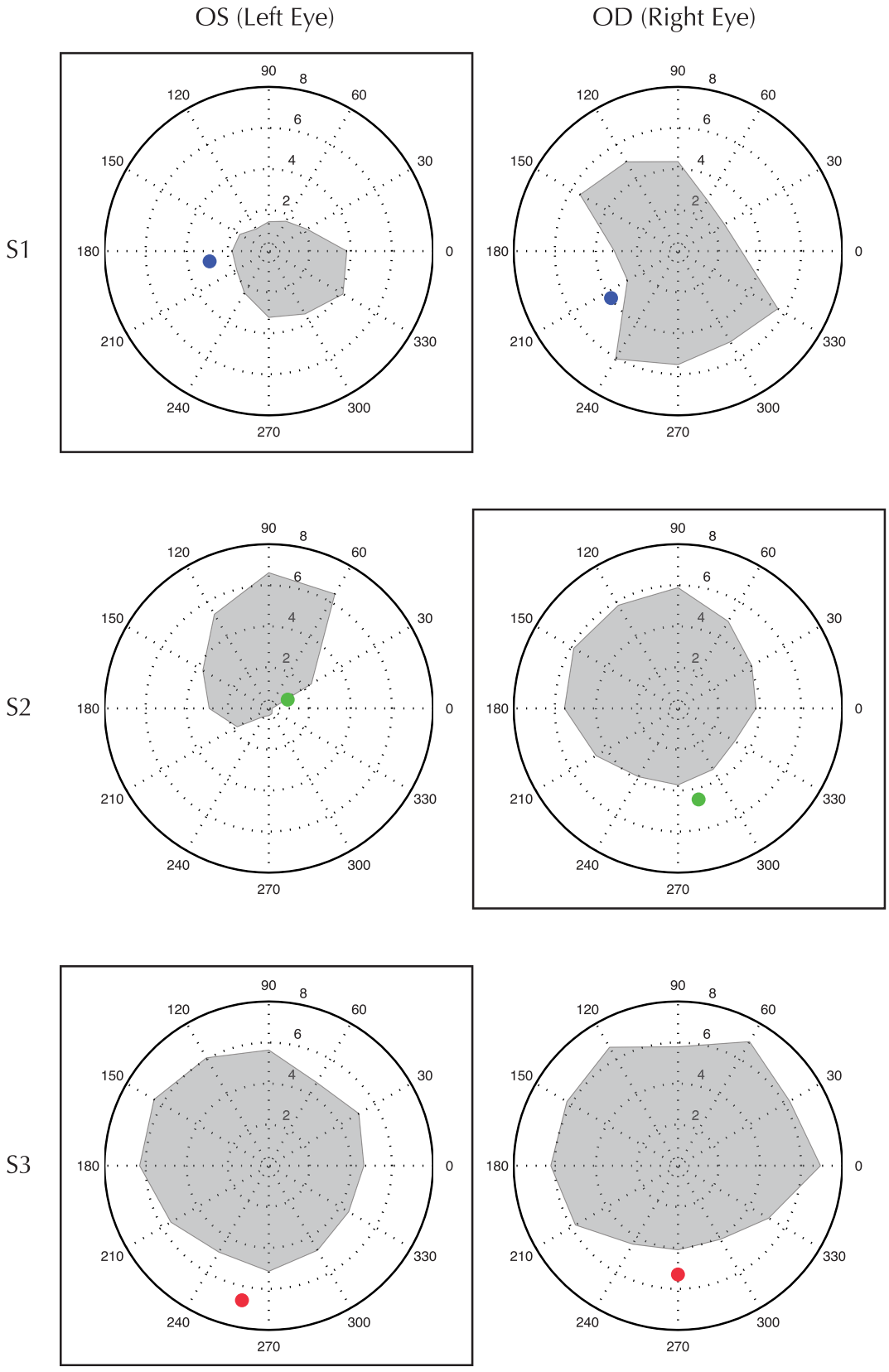

Figure 1. Locations of PRL (dots) and absolute central scotoma (shaded regions) in the visual field of each eye of the three AMD participants obtained monocularly using the SLO. The preferred eye for each AMD participant is indicated by a surrounding rectangle.

	AMD patient	Elderly control	Young control
Eccentricity: 2.93			
ID	S1 (AMD)	GA	RM
Age	73	70	31
Sex	F	F	F
Eccentricity: 4.55°			
ID	S2 (AMD)	RB	TC
Age	82	66	20
Sex	F	M	F
Eccentricity: 6.74°			
ID	S3 (AMD)	RC	BF
Age	85	75	32
Sex	M	M	M

Table 2. The PRL/testing eccentricity, age, and sex of the AMD participants and the corresponding elderly and young controls.

on self-report, which, for two of the three participants, corresponded to the eye with better acuity. In AMD, binocular and monocular acuity and fixation stability measured from the better-seeing eye typically do not differ although this is not the case for the worse-seeing eye (Tarita-Nistor, Brent, Steinbach, & González, 2011). We further assumed that the PRL a participant used in the experiment was the same one that we obtained with SLO although currently there is no technology that allows us to ascertain whether or not this is indeed the case.

For testing the AMD participants at Berkeley, stimuli were presented on a Sony color graphic display (model GDM-F500R; resolution: 1280 × 1024 at 75 Hz) and controlled by custom-written software in MATLAB on a Macintosh Intel Macbook computer. For the control participants at USC, stimuli were displayed on a Dell P1230 19-in. CRT monitor (resolution: 1024 × 768 at 85 Hz) at a viewing distance of 57 cm and controlled using a custom-built desktop running Windows 7 Enterprise. At both Berkeley and USC, a grayscale video attenuator (Li, Lu, Xu, Jin, & Zhou, 2003) was used with custom-built contrast calibration and control software implemented in MATLAB to provide 11 bits of linearly spaced contrast levels. To minimize any effect due to luminance inhomogeneity of the displays, the target object was always presented at the physical center of the displays.

Practice

All participants were given a brief period of practice to familiarize themselves with the object set—the set of images to be presented and the corresponding labels. For the AMD participants, this was done at the start of every session with feedback from the experimenter. All objects were presented individually, one by one, on a display screen, and the name given to the object was read out using the computer speech function. Participants were allowed to go through this phase as many times as they wanted throughout each testing session, typically two to four times. During testing, the participants would sometimes respond with a different term that had the same meaning (e.g., "water bottle" instead of "jug"). In those cases, the response was scored as correct as this was a test of their object recognition ability, not their memory or how an object was named in the experiment. The task was generally effortful for these participants, and some objects were more challenging than others.

For control participants, the practice was done via a computer program implemented in MATLAB, first at the fovea with natural gaze, then in the periphery. Objects were presented at the maximum contrast that avoided luminance clipping and were larger than the size that would be presented in the experiment. All objects were presented randomly in one block, and this was repeated for at least two blocks in the central vision and three blocks in the peripheral location until 100% recognition performance was attained. They were then followed by a further training phase in which the objects were presented in the peripheral location, and contrast thresholds for 75% correct identification were estimated using QUEST (Watson & Pelli, 1983) as implemented in the Psychophysics Toolbox (version 3.0.8). This included 50 trials per block in which objects were selected from the set randomly with at least five consecutive blocks presented to attain a stable threshold region. Following this initial brief practice period, participants were refamiliarized with the object set at full contrast and the corresponding labels prior to starting a new session.

Main experiment

In each trial, the participant viewed the stimulus for as long as they required before indicating that they were ready to respond. The young controls did this by pressing the space bar, and the elderly controls and AMD participants verbally identified the target. The names of the 20 possible target objects were then presented on screen for controls, and for the AMD participants, the pictures of all objects were presented. For the AMD participants and elderly controls, the experimenter selected the object that the participant had identified at the end of the trial. The young control participants selected their choice by computer mouse click of an object name.

For each trial, the target object was presented at the center of the monitor. For AMD participants, they were instructed to look at the target with their PRL. For the control participants, a fixation mark was presented on the screen such that, when fixating at the mark, the target would appear at the peripheral

location corresponding to the PRL of the paired AMD participant. The stimulus was temporarily removed whenever fixation deviated from the fixation mark by more than 1.5° in any direction. This fixation-contingent procedure allowed a control subject to view the stimulus at the intended eccentricity for as long as needed (Wallace, Chiu, Nandy, & Tjan, 2013).

The target contrast was manipulated trial by trial according to the QUEST procedure with 50 trials per spacing to converge at the 75% correct identification. This performance level was used for both AMD participants and the paired controls. Seven target–flanker spacings were used, logarithmically spaced in the region bracketing the predicted critical spacing value. The spacings specified the distance between the centers of the target and flanker objects. One spacing was used per block of 50 trials, and spacings were randomly assigned to each block. For the control participants, the fixation mark was presented 250 ms before target presentation and was preceded by an alert beep to demand the participants reorient their eyes and get ready. There was a 750-ms interval between each trial. For the AMD participants, fixation period was 1 s, and the intertrial interval was also 1 s. Each block began with 10 practice trials that were discarded in the analysis.

Eye tracking

For control participants, eye movements were monitored monocularly using the Eyelink 1000 Tower Mount (SR Research) while participants viewed the stimulus binocularly. Participants were instructed to adjust the seat height to find a comfortable position, and headrest height was also manipulated to ensure comfort for participants. Camera position and focus was manipulated if necessary. In most cases, auto-thresholds were appropriate for establishing accurate tracking of pupil and corneal reflection. Eye-tracker calibration preceded each block of trials using a standard nine-point target grid to map the eye data to gaze position. Online gaze position was used to gate stimulus presentation; the stimulus was presented on screen at a specified distance from the fixation mark only when the participant's (foveal) gaze was within a tolerance region of ±1.5° around the fixation cross. If a participant did not accurately fixate the fixation mark, presentation was withheld until accurate fixation resumed. This procedure ensured accurate control of stimulus eccentricity over unrestricted viewing durations.

Data analysis

Data analysis largely followed the method previously described in Wallace and Tjan (2011) and

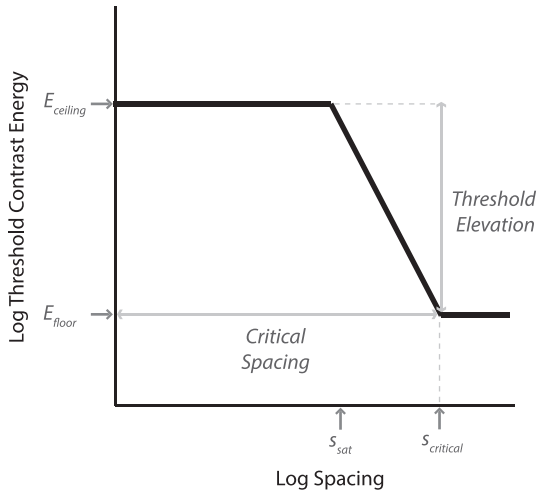

Figure 2. The threshold versus spacing function described in terms of four parameters ($E_{ceiling}$, E_{floor}, s_{sat}, $s_{critical}$), which, in turn, provides two key characterizations of crowding: critical spacing ($s_{critical}$) and threshold elevation ($E_{ceiling}/E_{floor}$). In addition, the floor threshold (E_{floor}) is used to compare peripheral form vision between AMD and normally sighted participants.

Wallace et al. (2013). For each spacing condition, we estimated threshold contrast energy, corresponding to 75% correct identification, by bootstrapping the raw per-trial data acquired with the QUEST procedure, for which contrast energy (E) of an object is the integral of squared Weber contrast over the entire object (Tjan, Braje, Legge, & Kersten, 1995). The data of threshold contrast energy (E) versus center-to-center spacing (s) were then fit with a clipped line function:

$$\log\Big(E(s)\Big) = \begin{cases} \log(E_{\text{ceiling}}) & \text{if} s \le s_{\text{sat}} \\ \log(E_{\text{floor}}) & \text{if } s \ge s_{\text{critical}} \\ \text{else} \\ \dfrac{\log(E_{\text{ceiling}}) - \log(E_{\text{floor}})}{\log(s_{\text{critical}}) - \log(s_{\text{sat}})}(\log(s_{\text{sat}}) - \log(s)) + \log\big(E_{\text{ceiling}}\big) \end{cases}. \quad (1)$$

This function (as shown in Figure 2) has four parameters: ceiling threshold contrast energy (E_{ceiling}), floor threshold contrast energy (E_{floor}), saturation spacing (s_{sat}), and critical spacing (s_{critical}). It provides an adequate description of the data. The part of the function in which spacing (s) is greater than s_{sat} is typically used to characterize crowding for relatively large target–flanker spacings (Chung et al., 2001; Pelli, Palomares, & Majaj, 2004; Wallace & Tjan, 2011). We estimated the parameters by fitting Equation 1 to the data of each participant using a multistart procedure, which minimizes the squared residual in log(E) and estimated the 95% (asymmetric) confidence interval of the four parameters (appendix B of Wallace & Tjan,

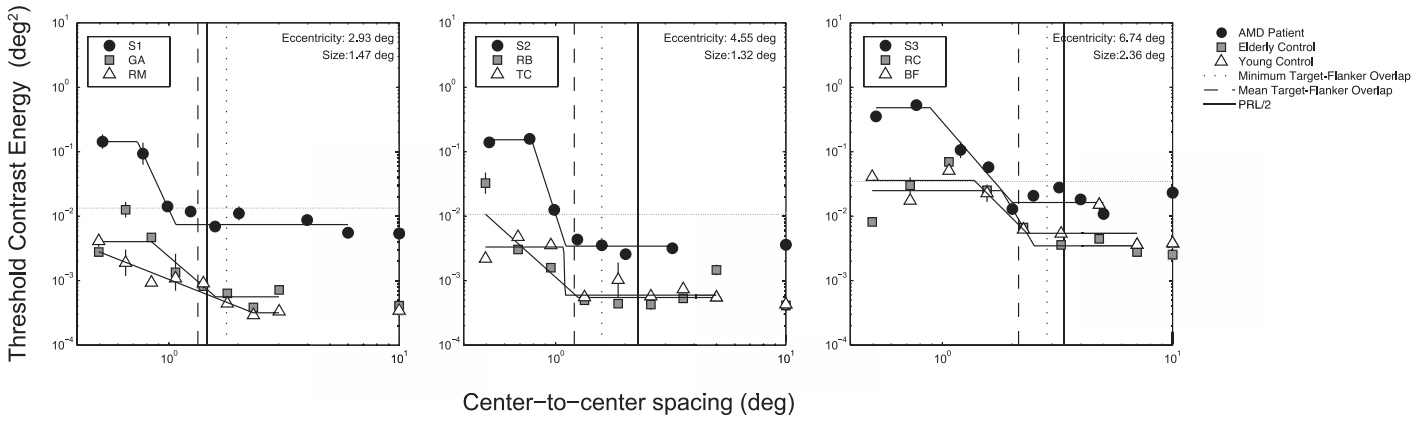

Figure 3. Threshold contrast energy as a function of center-to-center spacing. Each plot contains the data for an AMD participant and the two controls tested at the same retinal location as the AMD participant's PRL. The dotted and dashed vertical lines delineate the minimum and mean target–flanker spacings, respectively, when the target and flanker overlap. The solid vertical line specifies half the distance to the PRL (Bouma's scaling factor of 0.5). The dotted horizontal lines indicate the contrast energy of the flanker. The data points on the far *y*-axis are contrast threshold for single target objects in the absence of flankers (baseline performance). The target eccentricity and size for each AMD participant and the paired controls are specified in the upper right of each plot.

2011). Some participants (young control RM and elderly control RD) did not show a plateau at small spacing values, in which case the saturation spacing was undefined, and we defined the ceiling threshold contrast energy as the estimated threshold obtained by the fitting function at the smallest spacing tested. When making comparisons of estimated parameters between a matched pair of participants, we determined significance at $\alpha = 0.05$ if and only if neither of the quantities was within the 95% bootstrapped confidence intervals of the other.

Results

There are three key aspects of our results that we discuss in turn: (a) critical spacing, (b) floor (non-crowded) threshold contrast energy, and (c) threshold elevation. Critical spacings across all participants were generally similar (Figures 3 and 4). Relative to the target eccentricity, the mean normalized critical spacings (center-to-center target–flanker spacing divided by target eccentricity) are AMD = 0.30 (SD = 0.06), Elderly Control = 0.40 (SD = 0.14), Young Control = 0.46 (SD = 0.29). These estimates are close to but generally smaller than the Bouma's law value of 0.5, consistent with the literature (Whitney & Levi, 2011) and a previous study of object crowding in normally sighted subjects (Wallace & Tjan, 2011). It is also worth noting that for two of the three AMD participants (S2 and S3), the PRL was almost directly below the anatomical fovea (Figures 1 and 7); thus, the target–flanker orientation was tangential at the PRL, which typically leads to a smaller critical spacing. This may explain why S1 had a similar crowding extent as S2 despite S1's PRL being at a smaller eccentricity and why the controls paired to S1 exhibited a larger crowding extent compared to those paired to S2. The larger difference between the control groups is in line with the finding by Chung (2013) that the reduced crowding at the PRLs of AMD observers was mostly along the radial direction. Also of note is the lack of a clear effect of age in the non-AMD control participants on this key feature of crowding—

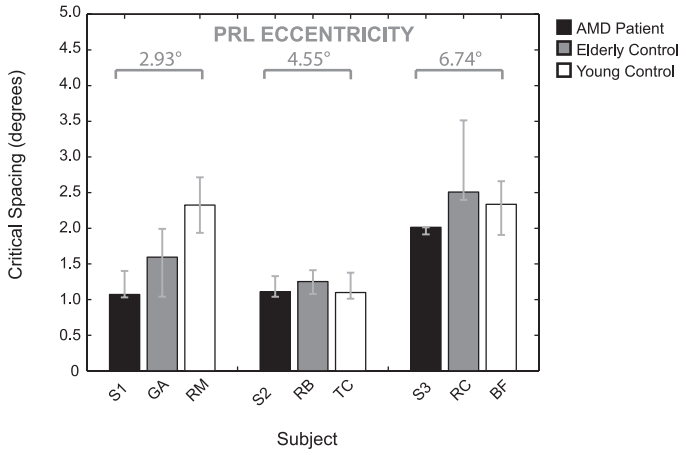

Figure 4. Critical spacings. The data are grouped according to the PRL/target eccentricity (the bracketed numbers) at which the AMD participants and the paired controls were tested. Error bars present bootstrapped 95% confidence intervals, which are generally asymmetric. Compared to the paired controls within each group, AMD participants had numerically smaller critical spacing, but this difference did not reach statistical significance except for S3 versus RC.

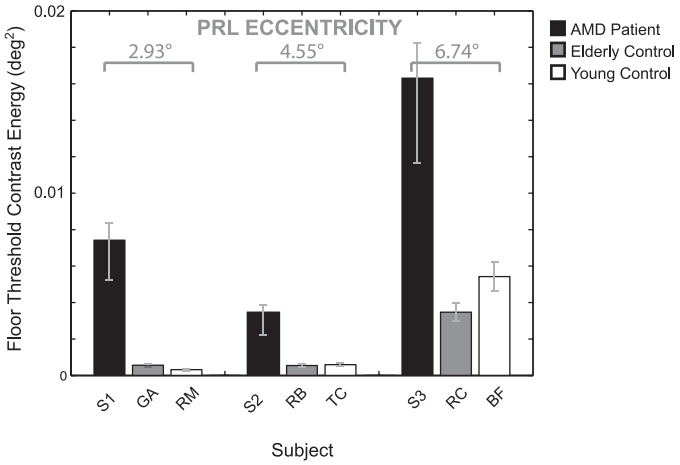

Figure 5. Floor threshold contrast energies. The data are grouped according to the PRL and target eccentricity (the bracketed numbers) at which the AMD participants and the paired controls were tested. Error bars present bootstrapped 95% confidence intervals on the fitted floor values, which are generally asymmetric. Floor (i.e., noncrowded) threshold level is significantly worse for the AMD participants at all eccentricities compared to both the elderly and young controls.

no deterioration nor improvement between the young and elderly controls.

Similarly, although the critical spacings of all three AMD cases are numerically smaller than the paired controls, there was no significant difference between AMD participants and controls matched to eccentricity. With a larger sample size (11 participants with macular disease), Chung (2013) found that, at the population level, the critical spacing as assessed with letter stimuli at PRL is smaller along the radial direction. For our AMD participants, the critical spacing value was similar to the mean distance of target–flanker overlap (long dashed line in Figure 3), meaning that, for objects, performance was relatively unaffected by target–flanker spacing until the target and flankers physically overlapped. We should note that when the target and flankers overlapped, the target was made to occlude the flankers. Hence, the target was always fully visible, and the observed threshold elevation cannot be attributed to overlap masking.

Although there is no apparent effect of critical spacing between the groups of participants, there is a clear difference in the contrast-energy thresholds for the AMD group. The entire threshold function was raised upward (Figure 3); floor thresholds are significantly higher (by confidence intervals; see Methods) than both the young and elderly controls (Figure 5). Mean floor threshold contrast energy (degrees squared): AMD = 0.0072 (SD = 0.0052), Elderly Control = 0.0015 (SD = 0.0017), Young Control = 0.0021 (SD = 0.0029). This indicates that, although there was no substantial effect of aging per se on contrast thresholds for object identification, the AMD participants had a harder time seeing the objects and require a much higher contrast to achieve a base level of performance. AMD participants required approximately two times the contrast (four times the contrast energy) as compared to controls to reach the 75% correct accuracy criterion at large target–flanker separation.

Further, for target–flanker spacings less than the critical spacing, there appears to be a cost over and above the difficulty the AMD participants had in seeing the noncrowded objects with or without flankers. The threshold functions are not simply vertically displaced relative to those of normal young and elderly controls; they are also stretched vertically. The threshold elevations (ratios of ceiling to floor thresholds) of the AMD participants are significantly higher overall (by confidence intervals; see Methods) than both the matched elderly and young controls (Figure 6) by about 0.5 log units (a factor of three). Mean contrast-energy threshold elevations in log units: AMD = 1.47 (SD = 0.18), Elderly Control = 1.04 (SD = 0.22), Young Control = 0.83 (SD = 0.10). In other words, crowding has a more detrimental effect on performance for the AMD participants even though the critical spacings for crowding are similar to those measured from the controls.

Discussion

Crowding, as quantified in terms of critical (center-to-center) spacing and threshold elevation, was measured for three AMD participants with well-defined PRL. Although numerically smaller, critical spacing for these AMD participants was not substantially different from that of aged-matched and young controls who were tested at the same peripheral location as the PRL of the paired AMD participants with unrestricted viewing time. However, we discovered that the AMD participants exhibited a clear deficit in contrast sensitivity for object identification. Contrast threshold in the noncrowded condition (i.e., floor threshold contrast energy) as well as threshold elevation due to crowding both appear to be significantly worse for the AMD participants as compared to controls. Figure 7 depicts the key findings with the AMD participants by illustrating the sizes of the test objects, the estimated critical spacings, and the target threshold contrast at critical spacings.

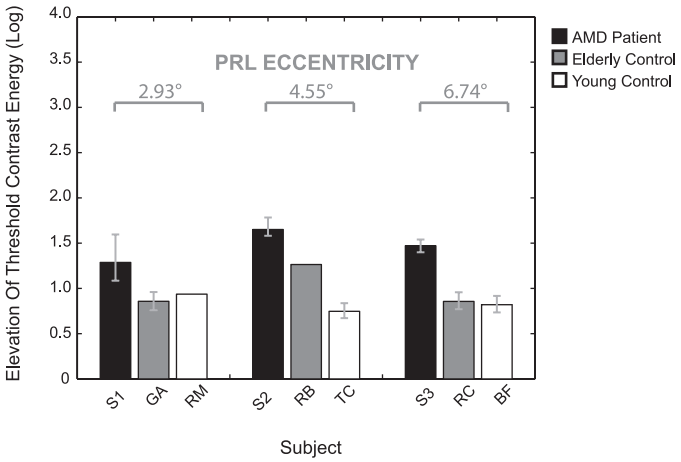

Figure 6. Threshold contrast energy elevations. The data are grouped according to the PRL/target eccentricity (the bracketed numbers) at which the AMD participants and the paired controls were also tested. Error bars present bootstrapped 95% confidence intervals, which are generally asymmetric. Error bars were omitted from RM and RB, who did not show saturation within the tested range of spacing (see Methods). Compared to the paired controls within each group, AMD participants had significantly higher threshold elevation (by about half of a log unit in terms of contrast energy) than the normally sighted controls regardless of the age of the controls.

To the best of our knowledge, the current study is the first attempt to measure the full threshold versus spacing functions for the quantification of object (not letter) crowding in AMD participants with a stable PRL and compare these directly with both normally sighted elderly and young controls. For elderly controls, inhibiting eye movements while attempting to maintain covert attention can be demanding. We were able to obtain reliable threshold measurements in elderly control participants by using a fixation-contingent stimulus presentation paradigm to withdraw the stimulus whenever fixation was not maintained. The same setup also allowed unrestricted viewing duration and thus facilitates direct comparisons between AMD and normally sighted control participants.

Spatial extent of crowding in AMD

Despite years of adaptation after the loss of central vision, the spatial extent of crowding appears to persist and does not substantially differ from that of controls—at least for the target–flanker orientations tested in the present study. Further, there was no evidence that an AMD observer, such as S1 (see Figure 7), could use her scotoma to block out a flanker and thus reduce crowding. The mean spatial extent of crowding for the AMD participants was 0.3 times target eccentricity (Figure 4), not significantly different from a ratio of 0.4 for the elderly or 0.46 for the young controls. These ratios are well within the range of crowding extents reported in the literature. Our previous study of crowding with objects, using normally sighted young adults and smaller objects, had obtained a mean extent of 0.35 times target eccentricity (Wallace & Tjan, 2011).

For normally sighted observers, the peripheral crowding zone is typically elliptical with the major

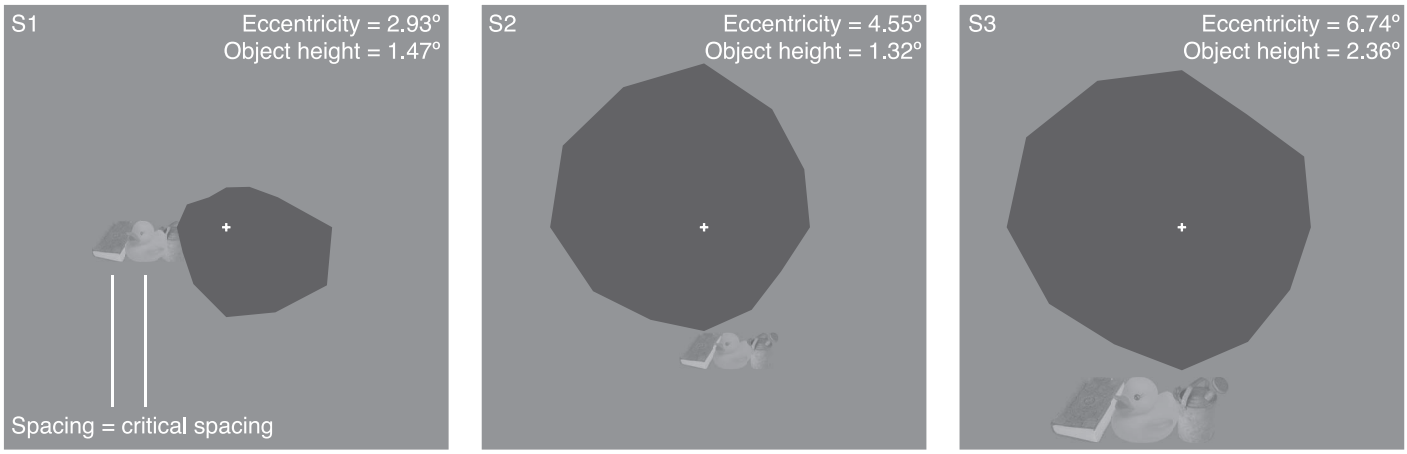

Figure 7. Illustrations of the key findings with the AMD participants. Different eccentric locations were used by the three AMD participants (S1, S2, and S3), corresponding to their PRLs in their preferred eyes. The dark patches represent the estimated absolute scotoma of the preferred eye of each AMD participant to illustrate the general visibility of the stimulus. In each panel are the depicted target and flanker contrasts, stimulus size and spacing that correspond to the target threshold contrast at critical spacing, the fixed flanker contrast, the stimulus size used, and the critical center-to-center spacing, respectively, for each of the three AMD participants. For the AMD participants, target and flankers lightly overlapped at critical spacing. By design, a target always occluded the flankers whenever they overlapped.

axis extending along the radial direction that connects the target and the fovea (Toet & Levi, 1992). In a previous study, we found that viewing duration in excess of 250 ms does not substantially affect critical spacing along the radial direction, and similar to our AMD participants, we found no evidence of normally sighted observers using a simulated scotoma advantageously to occlude any flanker (Wallace et al., 2013).

In a larger study than the present work, and using letters, Chung (2013) found a modest but significant reduction of critical spacing at the PRL in AMD patients compared to controls. Chung found that the reduction was mainly along the radial direction (the direction of the PRL with respect to the anatomical fovea), thus leading to a rounding of the crowding zone at the PRL. The same study found no change in the critical spacing along the tangential direction. This suggests an underlying plasticity to the spatial effects of crowding but that certain components of crowding may not be malleable to experience. Nandy and Tjan (2009, 2012) provide a model that determines the shape of the crowding zone in terms of the image statistics generated during eye movements by foveating saccades. Such movements are generally radially directed, driving the radial-tangential anisotropy. This model predicts that the altered image statistics associated with a central scotoma and an established PRL would drive the crowding zone at PRL to isotropy (Nandy & Tjan, 2012, supplement 4). The current study, using horizontally arranged flankers, measured only one dimension of the two-dimensional structure of the crowding zone. For two participants (S2, S3) with a PRL directly beneath the natural fovea in the visual field, the critical spacing being measured was along the tangential direction. That we did not find any significant reduction in critical spacing for these two AMD participants is consistent with Chung (2013).

We note that there were a number of differences between the two studies: Chung (2013) measured monocular crowding with letters using an SLO, and the current study measured binocular crowding with objects on a conventional CRT. Nevertheless, there is no reason to believe that the two studies are fundamentally different. Indeed, the mean crowding extent at the PRLs of Chung's (2013) participants with macular disease was 0.4 times the target eccentricity ($SD = 0.1$) measured with letters, which is similar to our value of 0.3 measured with objects.

Contrast-sensitivity deficits in AMD

Our results show that the functional vision for object recognition at the PRL of an AMD observer is worse than that of a normally sighted individual. Contrast-energy thresholds for object identification without crowding was more than four times higher for AMD participants relative to controls. Most patients with AMD suffer from contrast deficits (Wolkstein, Atkin, & Bodis-Wollner, 1980; Marmor, 1986; Sunness et al., 1997; Mei & Leat, 2007; Chung & Legge, 2016), so it is not surprising that they require higher contrast to identify objects. Moreover, the PRL is often close to the edge of the absolute scotoma and thus further affected by the macular pathology. Although these data suggest that the PRL might be in a zone of relative scotoma, the fact that the participants stuck to it under the unrestricted free-viewing condition suggests this retinal locus had high utility for some reason that is currently still unknown to us.

In addition to the greatly elevated noncrowded threshold, we also observed a larger threshold elevation for the AMD participants as compared to controls, which is indicative of a contrast deficit associated with crowding (Coates, Chin, & Chung, 2013). Specifically, crowding elevated contrast threshold energy by a factor of 30 in AMD participants as compared to a factor of 10 or less in the age-matched controls. The core reason for this exaggerated effect of crowding is not clear. This difference cannot be attributed to a lack of binocular summation in AMD participants (about a factor of two in energy units in normally sighted observers: Legge, 1984). Binocular suppression (Pardhan & Gilchrist, 1991) is unlikely to be a cause as binocular acuity in AMD is typically similar to the monocular acuity measured from the better eye (Tarita-Nistor et al., 2011).

We previously found that with normal vision, the critical spacing for object crowding was very similar to that for letter crowding, but the contrast threshold elevation associated with object crowding was much lower; observers required a smaller increase in contrast to counteract crowding with objects than with letters. In the case of participants with normal vision, it appears that the informative features of an object, defined by local continuous variation in contrast, mitigate the detrimental effects of crowding (Wallace & Tjan, 2011). In the case of AMD participants, even with a well-developed PRL, this advantage of objects is apparently lost. Although the extensive practice associated with a stable PRL can lead to a reduced crowding zone in AMD observers (Chung, 2013, 2014), the contrast deficit in AMD is apparently insurmountable and particularly damaging to performance in crowded conditions. Digital image-contrast enhancements have been proposed as a visual aid for individuals with low vision, including those with macular degeneration with documented benefits (Peli, Goldstein, Young, Trempe, & Buzney,

1991; Choudhury & Medioni, 2010; Kwon et al., 2012; Satgunam et al., 2012).

Object size and between-objects crowding

The object-size threshold of the AMD participants was indistinguishable from that of the normally sighted elderly participants: eccentricity-normalized AMD size threshold at PRL (object size at threshold divided by eccentricity) = 0.20 ($SD = 0.08$) and normalized size threshold for age-matched controls = 0.25 ($SD = 0.07$). However, the AMD participants required considerable effort to perform this task. To compensate for this and to facilitate data collection, the object size we used in the experiment was twice the AMD participant's size thresholds.

The need for using larger objects in our experiment mirrors the most common method to compensate for deficits of contrast sensitivity in daily activities: using a magnifier. We do not think that our practical need for using larger objects in the experiment prevented us from measuring critical spacing smaller than the mean object size. This is because crowding mostly depends on center-to-center spacing, not the gap between objects (Levi, 2008; Pelli & Tillman, 2008). In our experiment, when the target and flankers overlapped, the target was made to occlude the flankers. At the estimated critical spacings, the target only slightly occluded the flankers (see Figure 7 for an illustration), and contrast threshold continued to deteriorate at smaller target–flanker spacings. Having the target occlude the flankers did not protect the target from clutter or crowding and did not lead to an underestimated crowding zone.

Although we presented the target in front of the flankers to avoid it being occluded, one may expect that close proximity of the flankers to the target could lead to surround suppression in addition to crowding (Petrov, Popple, & McKee, 2007). Data from the controls argue against this possibility; the controls were tested with the same object sizes as the AMD participants and achieved similar critical spacings. Critically, however, threshold elevations for the controls with target–flanker overlaps were comparable to an earlier study using smaller object sizes, which avoided target–flanker overlap at critical spacing (Wallace & Tjan, 2011).

A modest amount of target–flanker overlap may reduce visibility of the bounding contour of the target object, but it has little qualitative impact on object identification. This is quite understandable. A typical object is rich in internal features, which allow it to be identified from a partial view. In Wallace and Tjan (2011), we show that masking the objects with a circular aperture, such that only the central region of an object was visible, did not affect critical spacing as compared to that obtained with whole objects. The same (null effect) was also observed for the complementary condition, in which the central region of an object was masked such that objects could only be identified by their bounding contours and internal features nearby.

Gaze instability

Because the PRL is often near the border of the central scotoma, gaze instability could move a target in and out of the scotoma and thus elevate contrast threshold. We did not measure fixation stability in our AMD participants, who viewed the stimuli binocularly, during the experiment. We had measured their fixation stability in monocular viewing with their preferred eye (Table 1), which should be similar to fixation stability with binocular viewing (Tarita-Nistor et al., 2011, 2012). In the better eyes of our participants, the typical distance between the PRL and the border of the absolute scotoma was about 1° (Figure 1), and the mean radius of the target objects were between 0.7° and 1.2° (Figure 3). The standard derivation of fixation in the relevant direction ranges from 0.33° (S3) to 0.95° (S1) (Table 1). Hence, gaze instability is a probable factor in the observed contrast threshold elevation.

However, it is unclear if gaze instability has any additional effect on crowding. In a recent study with normally sighted participants (Wallace et al., 2013), we measured crowding in different gaze-control regimes, including a condition of unrestricted eye movements, with the minimal target eccentricity limited by an artificial central scotoma and the fixation-contingent condition used with the control participants in the current study. These two conditions differed greatly in terms of gaze variability. However, we found no difference in the spatial extent of crowding between the two when we expressed the spatial extents of crowding in terms of the effective target eccentricities in the corresponding conditions.

Conclusion

In summary, we found that the spatial extent of object crowding remains similar between AMD patients and controls tested at locations matching the patients' PRL. There is, however, a large contrast detriment on the ability of AMD patients to identify objects, which is exacerbated in conditions of crowding. We thus suggest that remedial programs and technologies for macular degeneration patients should focus on contrast enhancement or reduction.

Keywords: crowding, form vision, peripheral vision, central vision loss

Acknowledgments

We dedicate this paper to our dear friend and colleague, Bosco Tjan, who passed away due to a tragic incident on December 2, 2016, after this paper had been sent to production. This work was supported by NIH/NEI Grants R01-EY017707 and R01-EY012810.

Commercial relationships: none.
Corresponding author: Susana Chung.
Email: s.chung@berkeley.edu.
Address: School of Optometry, University of California, Berkeley, Berkeley, CA 94720-2020, USA.

References

Andriessen, J. J., & Bouma, H. (1976). Eccentric vision: Adverse interactions between line segments. *Vision Research, 16*(1), 71–78.

Bouma, H. (1970, Apr 1). Interaction effects in parafoveal letter recognition. *Nature, 226*(5241), 177–178.

Bouma, H. (1973). Visual interference in the parafoveal recognition of initial and final letters of words. *Vision Research, 13*(4), 767–782.

Calabrèse, A., Bernard, J. B., Hoffart, L., Faure, G., Barouch, F., Conrath, J., & Castet, E. (2010). Small effect of interline spacing on maximal reading speed in low-vision patients with central field loss irrespective of scotoma size. *Investigative Ophthalmology and Visual Science, 51*, 1247–1254. [PubMed] [Article]

Choudhury, A., & Medioni, G. (2010). Color contrast enhancement for visually impaired people. In *2010 IEEE Computer Society Conference on Computer Vision and Pattern Recognition - Workshops* (pp. 33–40). New York: IEEE.

Chung, S. T. L. (2013). Cortical reorganization after long-term adaptation to retinal lesions in humans. *The Journal of Neuroscience, 33*(46), 18080–18086.

Chung, S. T. L. (2014). Size or spacing: Which limits letter recognition in people with age-related macular degeneration? *Vision Research, 101*, 167–176.

Chung, S. T. L., Jarvis, S. H., Woo, S. Y., Hanson, K., & Jose, R. T. (2008). Reading speed does not benefit from increased line spacing in AMD patients. *Optometry and Vision Science, 85*, 827–833.

Chung, S. T. L., & Legge, G. E. (2016). Comparing the shape of the contrast sensitivity functions for normal and low vision. *Investigative Ophthalmology and Visual Science, 57*, 198–207.

Chung, S. T. L., Levi, D. M., & Legge, G. E. (2001). Spatial-frequency and contrast properties of crowding. *Vision Research, 41*, 1833–1850. [PubMed] [Article]

Coates, D. R., Chin, J. M., & Chung, S. T. L. (2013). Factors affecting crowded acuity: Eccentricity and contrast. *Optometry and Vision Science, 90*(7), 628–638.

Cummings, R. W., Whittaker, S. G., Watson, G. R., & Budd, J. M. (1985). Scanning characters and reading with a central scotoma. *American Journal of Optometry and Physiological Optics, 62*(12), 833–843.

Farzin, F., Rivera, S. M., & Whitney, D. (2009). Holistic crowding of Mooney faces. *Journal of Vision, 9*(6):18, 1–15, doi:10.1167/9.6.18.

Flom, M. C., Heath, G. G., & Takahashi, E. (1963, Nov 15). Contour interaction and visual resolution: Contralateral effects. *Science, 142*(3594), 979–980.

He, S., Cavanagh, P., & Intriligator, J. (1996, Sept 26). Attentional resolution and the locus of visual awareness. *Nature, 383*(6598), 334–337.

Ikeda, H., Watanabe, K., & Cavanagh, P. (2013). Crowding of biological motion stimuli. *Journal of Vision, 13*(4):20, 1–6, doi:10.1167/13.4.20. [PubMed] [Article]

Kwon, M., Ramachandra, C., Satgunam, P., Mel, B. W., Peli, E., & Tjan, B. S. (2012). Contour enhancement benefits older adults with simulated central field loss. *Optometry and Vision Science, 89*(9), 1374–1384.

Legge, G. E. (1984). Binocular contrast summation—II. Quadratic summation. *Vision Research, 24*(4), 385–394.

Levi, D. M. (2008). Crowding—An essential bottleneck for object recognition: A mini-review. *Vision Research, 48*, 635–654.

Levi, D. M., Hariharan, S., & Klein, S. A. (2002). Suppressive and facilitatory spatial interactions in peripheral vision: Peripheral crowding is neither size invariant nor simple contrast masking. *Journal of Vision, 2*(2):3, 167–177, doi:10.1167/2.2.3. [PubMed] [Article]

Li, X., Lu, Z. L., Xu, P., Jin, J., & Zhou, Y. (2003). Generating high gray-level resolution monochrome displays with conventional computer graphics cards

and color monitors. *Journal of Neuroscience Methods, 130*(1), 9–18.

Louie, E. G., Bressler, D. W., & Whitney, D. (2007). Holistic crowding: Selective interference between configural representations of faces in crowded scenes. *Journal of Vision, 7*(2):24, 1–11, doi:10.1167/7.2.24. [PubMed] [Article]

Marmor, M. F. (1986). Contrast sensitivity versus visual acuity in retinal disease. *The British Journal of Ophthalmology, 70*(7), 553–559.

Martelli, M., Majaj, N. J., & Pelli, D. (2005). Are faces processed like words? A diagnostic test for recognition by parts. *Journal of Vision, 5*(1):6, 58–70, doi:10.1167/5.1.6. [PubMed] [Article]

Mei, M., & Leat, S. J. (2007). Suprathreshold contrast matching in maculopathy. *Investigative Ophthalmology & Visual Science, 48*(7), 3419–3424. [PubMed] [Article]

Nandy, A. S., & Tjan, B. S. (2007). The nature of letter crowding as revealed by first- and second-order classification images. *Journal of Vision, 7*(2):5, 1–26, doi:10.1167/7.2.5. [PubMed] [Article]

Nandy, A. S., & Tjan, B. S. (2009). The fine spatial structure of crowding zones. *Journal of Vision, 9*(8):1001, doi:10.1167/9.8.1001. [Abstract]

Nandy, A. S., & Tjan, B. S. (2012). Saccade-confounded image statistics explain visual crowding. *Nature Neuroscience, 15*(3), 463–469.

Pardhan, S., & Gilchrist, J. (1991). The importance of measuring binocular contrast sensitivity in unilateral cataract. *Eye, 5*(1), 31–35.

Patel, P. J., Chen, F. K., Rubin, G. S., & Tufail, A. (2008). Intersession repeatability of visual acuity scores in age-related macular degeneration. *Investigative Ophthalmology & Visual Science, 49*(10), 4347–4352. [PubMed] [Article]

Peli, E., Goldstein, R. B., Young, G. M., Trempe, C. L., & Buzney, S. M. (1991). Image enhancement for the visually impaired. Simulations and experimental results. *Investigative Ophthalmology & Visual Science, 32*(8), 2337–2350. [PubMed] [Article]

Pelli, D. G., Palomares, M., & Majaj, N. J. (2004). Crowding is unlike ordinary masking: Distinguishing feature integration from detection. *Journal of Vision, 4*(12):12, 1136–1169, doi:10.1167/4.12.12. [PubMed] [Article]

Pelli, D., & Tillman, K. (2008, Oct). The uncrowded window of object recognition. *Nature Neuroscience,* 1129–1135.

Petrov, Y., Popple, A. V., & McKee, S. P. (2007). Crowding and surround suppression: Not to be confused. *Journal of Vision, 7*(2):12, 1–9, doi:10.1167/7.2.12. [PubMed] [Article]

Satgunam, P., Woods, R. L., Luo, G., Bronstad, P. M., Reynolds, Z., Ramachandra, C., Mel, B. W., & Peli, E. (2012). Effects of contour enhancement on low-vision preference and visual search. *Optometry and Vision Science, 89*(9), E1364–E1373.

Schuchard, R. A., & Fletcher, D. C. (1994). Preferred retinal locus: A review with applications in low vision rehabilitation. *Ophthalmology Clinics of North America, 7*, 243–256.

Strasburger, H., Harvey, L. O., & Rentschler, I. (1991). Contrast thresholds for identification of numeric characters in direct and eccentric view. *Perception & Psychophysics, 49*(6), 495–508.

Sunness, J. S., Rubin, G. S., Applegate, C. E., Bressler, N. M., Marsh, M. J., Hawkins, B. S., & Haselwood, D. (1997). Visual function abnormalities and prognosis in eyes with age-related geographic atrophy of the macula and good visual acuity. *Ophthalmology, 104*(10), 1677–1691.

Tarita-Nistor, L., Brent, M. H., Steinbach, M. J., & González, E. G. (2011). Fixation stability during binocular viewing in patients with age-related macular degeneration. *Investigative Opthalmology & Visual Science, 52*(3), 1887–1893. [PubMed] [Article]

Tarita-Nistor, L., Brent, M. H., Steinbach, M. J., & González, E. G. (2012). Fixation patterns in maculopathy: From binocular to monocular viewing. *Optometry and Vision Science, 89*(3), 277–287.

Tjan, B. S., Braje, W. L., Legge, G. E., & Kersten, D. (1995). Human efficiency for recognizing 3-D objects in luminance noise. *Vision Research, 35*(21), 3053–3069.

Toet, A., & Levi, D. M. (1992). The two-dimensional shape of spatial interaction zones in the parafovea. *Vision Research, 32*, 1349–1357.

Wallace, J. M., Chiu, M. K., Nandy, A. S., & Tjan, B. S. (2013). Crowding during restricted and free viewing. *Vision Research, 84*, 50–59.

Wallace, J. M., & Tjan, B. S. (2011). Object crowding. *Journal of Vision, 11*(6):19, 1–17, doi:10.1167/11.6.19. [PubMed] [Article]

Watson, A. B., & Pelli, D. (1983). QUEST: A Bayesian adaptive psychometric method. *Perception & Psychophysics, 33*(2), 113–120.

Whitney, D., & Levi, D. M. (2011). Visual crowding: A fundamental limit on conscious perception and object recognition. *Trends in Cognitive Sciences, 15*(4), 160–168.

Wolkstein, M., Atkin, A., & Bodis-Wollner, I. (1980). Contrast sensitivity in retinal disease. *Ophthalmology, 87*(11), 1140–1149.